

High Performance Diode Lasers Emitting at 780-820 nm

L. Bao^{*}, M. DeVito, M. Grimshaw, P. Leisher[†], H. Zhou, W. Dong, X. Guan, S. Zhang, R. Martinsen, J. Haden

*n*Light Corporation
Vancouver, WA 98665, USA

ABSTRACT

High power 780-820 nm diode lasers have been developed for pumping and material processing systems. This paper presents recent progress in the development of such devices for use in high performance industrial applications. A newly released laser design in this wavelength range demonstrates thermally limited >25W CW power without catastrophic optical mirror damage (COMD), with peak wallplug efficiency ~65%. Ongoing accelerated lifetesting projects a time to 5% failure of ~10 years at 5 and 8 W operating powers for 95 and 200 μ m emitter widths, respectively. Preliminary results indicate the presence and competition of a random and wear-out failure mode. Fiber-coupled modules based on arrays of these devices support >100W reliable operation, with a high 56% peak efficiency (ex-fiber) and improved brightness/reliability.

Key words: Reliability, lifetime, lifetest, high power, high efficiency, 808 nm, 790 nm, semiconductor laser diodes, fiber-coupled modules

1. INTRODUCTION

High power diode lasers at 780-800 nm emission are used for many different applications, including solid-state laser pumping, Alkali vapor laser pumping, and fiber laser pumping [1-5]. Such devices are also needed for materials processing area, such as laser marking, welding, and consumer electronics manufacturing. These applications have increased the output brightness requirements for diode lasers. For example, high-brightness pumps are used in end-pumped solid state lasers in order to increase overlap of the pump area with the fundamental cavity mode, thereby increasing the total power scalability. High power and high brightness pump laser sources at 790 nm are especially needed, for kW-class Tm-doped fiber lasers [4-5]. The developments in the last decade have greatly improved diode laser performance and reliability [6-16]. For example, wall plug efficiencies in excess of 70% have been reported for diodes operating in the 9xx nm wavelength range as the result of efforts such as Super High Efficiency Diode Sources (SHEDS) program funded by DARPA [7]. However, due to high photon energy (and the associated efficiency and reliability implications) the development of high power/brightness 780-800 nm light sources has lagged.

This paper reports new progress on single emitter broad area devices from 780 nm to 820 nm wavelength region. High performance high efficiency (HE) diode lasers for rated output powers of 5 and 8 W were developed. Their operation power, efficiency, temperature performance, beam quality and lifetime will be presented. Failure modes in lifetest will be discussed and paths for reliability improvement will be addressed. Qualification results of fiber-coupled modules with these new developed lasers will be presented. Improved efficiency and power has been demonstrated.

2. 780-820 DIODE LASERS WITH HIGH EFFICIENCY (HE) DESIGN

Because industrial application normally require a more balanced laser quality in terms of high power, high brightness, high efficiency, good beam quality, good temperature performance and required reliability, our newly developed high efficiency (HE) design of high power lasers at 780 nm to 820 nm wavelength sought to balance the various performance metrics. The HE design utilized a super large optical cavity (SLOC) structure design, in order to increase both operation power and reliability by reducing optical power density on the facet. The SLOC design also enables long cavity length

^{*} ling.bao@nlight.net; phone 360.566.4460; <http://www.nlight.net>

[†]Dept. of Physics and Optical Engineering, Rose-Hulman Institute of Technology, Terre Haute, IN 47803

and lower operation current density by reducing internal loss, to further improve operation power and reliability. This design also combines a refined layer composition from a hybrid material system and doping concentration tuning to achieve both good carrier confinement and low voltage defect. The same approach has enabled 9xx nm lasers with >14W reliable operation [15-16], for devices with 95 μm stripes and 3.8 mm cavity lengths.

The epitaxial structure is grown by low pressure Metal-Organic Chemical Vapor Deposition, and the wafers are processed for good near field and far field control. All laser devices are passivated (*n*XLT). Laser bars are cleaved and low/high reflectivity dielectric mirrors are deposited on front/rear facets. After coating, bars are cleaved into single emitter chips with 95 μm stripes and 200 μm stripes, 3.8mm cavity lengths. The chips are bonded p-side down with AuSn solder onto expansion-matched heatsinks. Every single device is subjected to multiple inspection processes, plus a test, burn-in, and test screening. Calibration of measured power and efficiency is NIST-traceable, and all voltage and resulted wall plug efficiency reported here were directly measured from the devices, without subtracting package-associated resistances.

2.1 Diode laser performance

The typical light versus current (LI) and wall-plug efficiency versus current of the HE devices are shown in Figure 1 (a) and (b), emitting at 808 nm and 790 nm separately, at a test station controlled temperature of 25 $^{\circ}\text{C}$. There are 10 devices in each plot, with the same configuration of 95 μm stripes and 3.8 mm cavity lengths. The slope efficiencies of these devices are around 1.29 W/A for 808 nm lasers, and 1.31 W/A for 790 nm lasers. Threshold currents are ~ 0.7 A. The peak wall plug efficiency of HE device is $\sim 65\%$. This high efficiency performance has been optimized for a wide wavelength range, from 780 nm to 820 nm [14], and is significantly improved over our previous generation product (58%). At 5 W, the operation current is ~ 4.5 A and wall plug efficiency is $\sim 64\%$, comparing favorably to similar structures designed for operation in the 9xx nm band [15-16]. Typical spectra are shown in Figure 2(a) and (b), for 808 nm and 790 nm separately, as a function of drive currents from 4 A to 8 A. At 5 A (5.5 W) and 25 $^{\circ}\text{C}$ operation, full-width half-maximum (FWHM) bandwidth is ~ 1.5 nm and full-width- $1/e^2$ (FW $1/e^2$) bandwidth is ~ 2.4 nm.

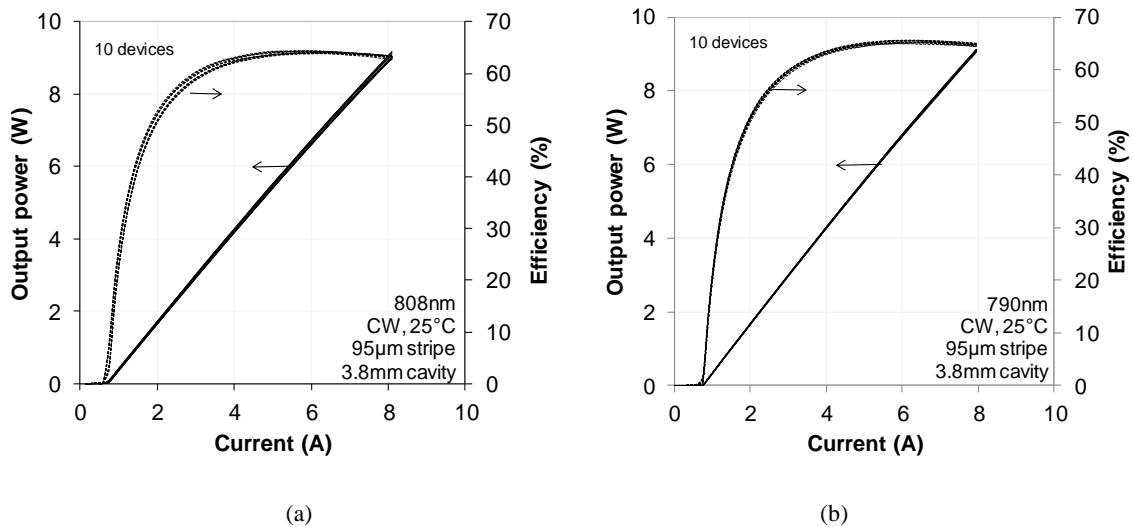
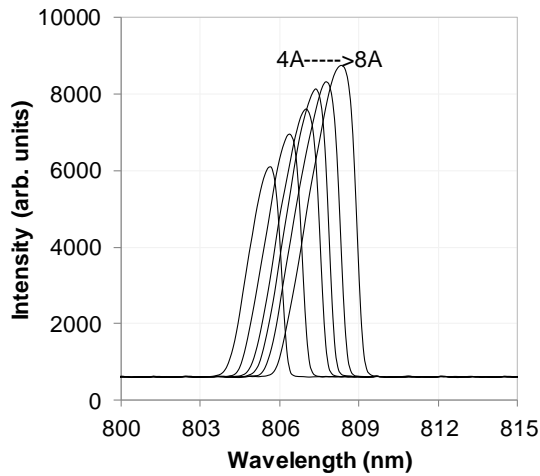
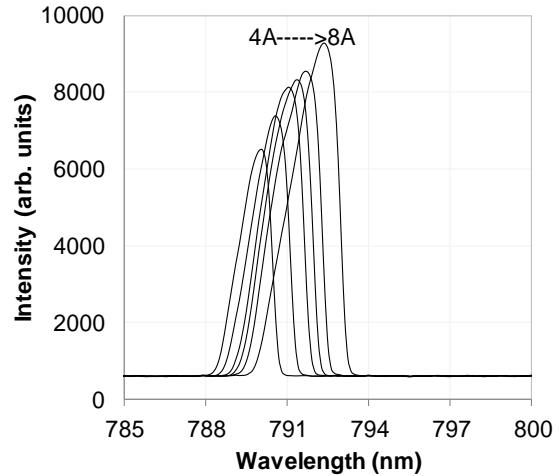


Figure 1: HE Lasers with 95 μm stripes and 3.8mm cavities, typical continuous wave (CW) optical power and wall-plug efficiency versus drive current operating at 25 $^{\circ}\text{C}$ for (a) 10 808 nm lasers (b) 10 790 nm lasers



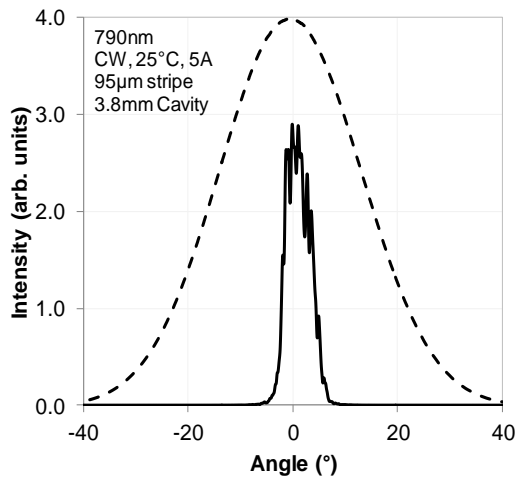
(a)



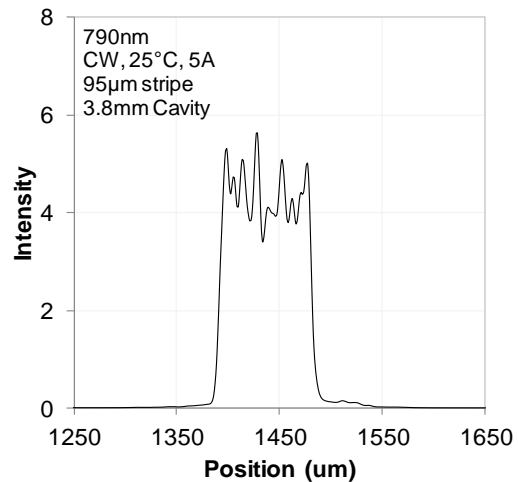
(b)

Figure 2: HE Lasers with 95 μm stripes and 3.8 mm cavities, typical spectrum with drive current from 4 A to 8 A operating at 25 $^{\circ}\text{C}$ for (a) 808 nm laser, (b) 790 nm laser

The slow-axis and fast-axis far fields of the HE 790 nm devices (in Figure 1) at 5 A (5.5 W) and 25 $^{\circ}\text{C}$ operation are shown in Figure 3(a). The FWHM and FW1/e² of the device fast-axis far field are about 32 $^{\circ}$ and 54 $^{\circ}$ respectively, while previous generation devices are 36 $^{\circ}$ and 62 $^{\circ}$, respectively. The FWHM and FW1/e² of the slow-axis far field are about 6.0 $^{\circ}$ and 8.2 $^{\circ}$, respectively. A typical slow-axis near field intensity profile as a function of position is shown in Figure 3(b). The FWHM and FW1/e² of the slow-axis near field are about 90 μm and 97 μm respectively.



(a)



(b)

Figure 3: HE 790 nm lasers with 95 μm stripe and 3.8 mm cavity (a) typical fast axis and slow axis far fields operating at 5 A 25 $^{\circ}\text{C}$ (b) typical slow axis near field at 5 A 25 $^{\circ}\text{C}$

Figure 4(a) contains LIV and wall-plug efficiency data of such HE device, with 200 μm stripes and 3.8 mm cavity lengths. There are 10 devices in the plot, emitting at 808 nm at a test station controlled temperature of 25 $^{\circ}\text{C}$. The slope

efficiencies of these devices are around 1.29 W/A, compared to 1.22 W/A of previous generation devices. Threshold current of the HE device was around 1.6 A. The peak wall plug efficiency of HE the device was about 63%. At 10W operation condition, the operation current and wall plug efficiency are 9 A and 63% respectively. Thermal rollover testing was performed on the HE devices. Figure 4(b) shows that the CW roll-over test at 10 °C cold plate control temperature. Rollover power was found to exceed 25W in all devices, a >20% increase over our previous generation structure. Catastrophic optical damage was not observed in the test. It is believed that this improvement will translate into improved device reliability.

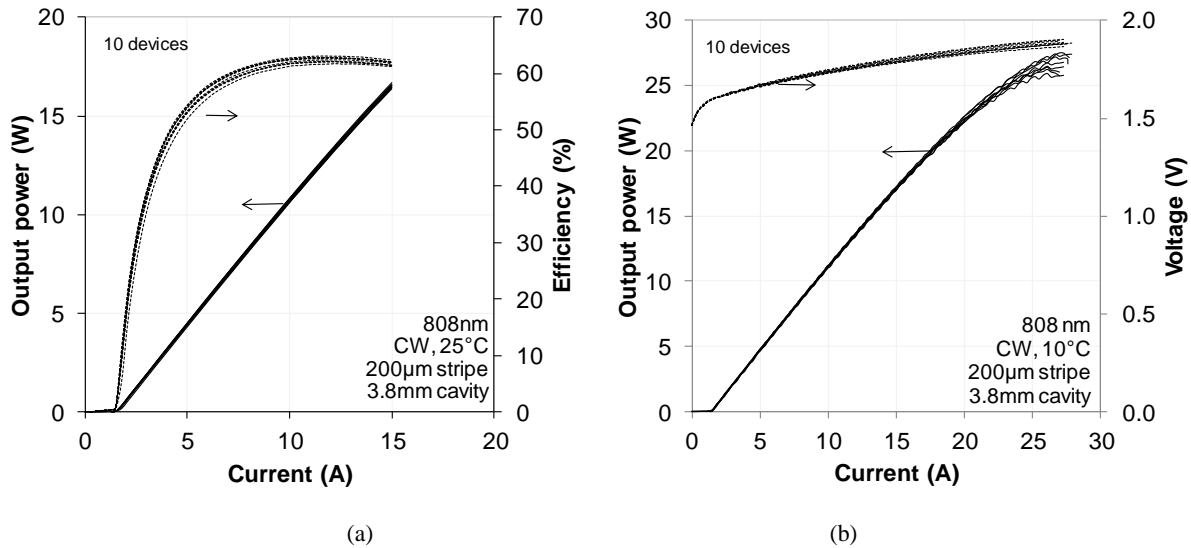


Figure 4: (a) CW LI and efficiency curves of HE structure devices at 25 °C; (b) CW LIV curves of HE structure devices at 10 °C, to power rollover;

2.2 Lifetest and reliability analysis

A total of 60 780-820 nm lasers with 95 µm stripes and 3.8 mm resonator length have been loaded for accelerated lifetest at 8 A and 50 °C heatsink temperature (junction temperature $T_j \sim 64$ °C). As seen in Figure 5(a), 20 ~790 nm devices have been lifetested for >4000 hours. Only one random failure was observed, however, there is a clear transition to a different failure rate after ~3000 hours. This failure mode is consistent with an increasing failure rate with time. Wear-out start is very common in high power 780-820 nm diode lasers. As a comparison in Figure 5(b), 40 ~808 nm devices have been life-tested for ~3500 hours, with two recent failures at ~3400 hours.

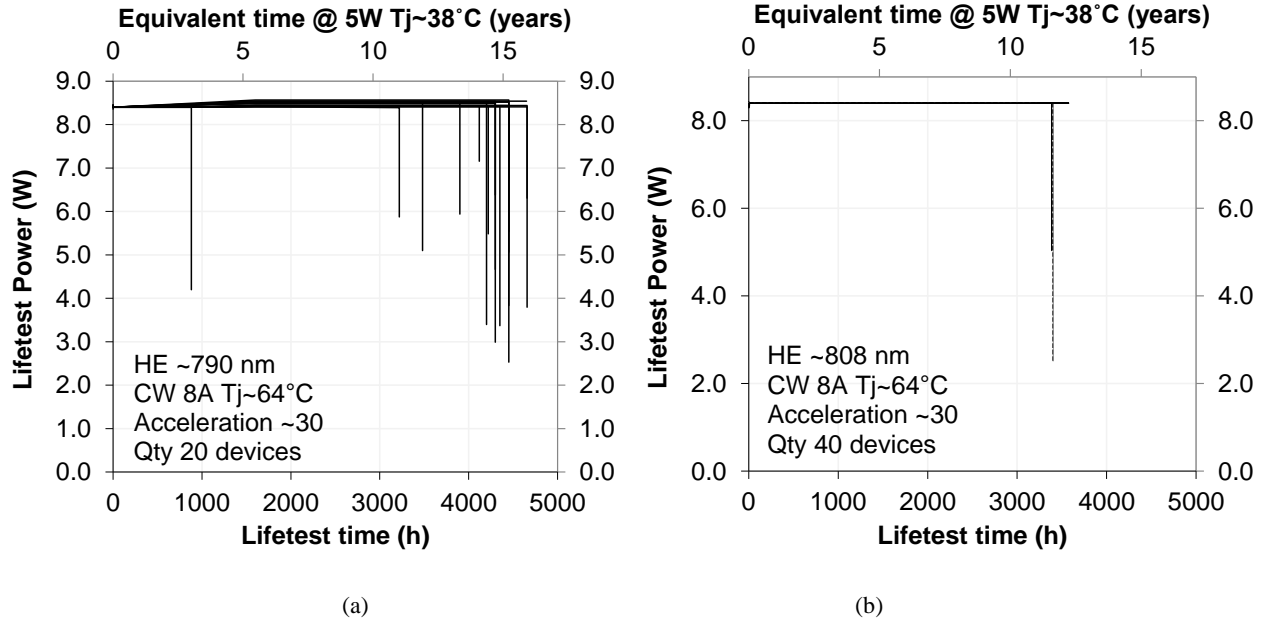


Figure 5: Accelerated lifetest at 8 A and 50 °C heatsink temperature (junction temperature $T_j \sim 64^\circ\text{C}$ on devices with 95 μm stripes and 3.8 mm cavities. (a) 20 790 nm devices, showing facet wear-out after 3000 hours accelerated lifetest, equivalent to >15 year at 5 W 25 °C (b) 40 808 nm devices with two failures observed at 3500 h.

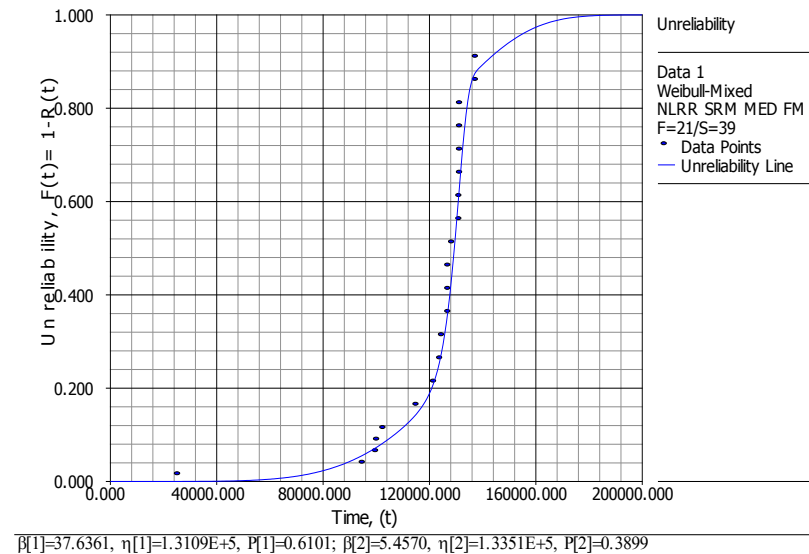
The acceleration model that is typically assumed for power and temperature acceleration is a combination of a power law (which describes the effective acceleration due to increasing optical power of the laser) and the Arrhenius law (which describes the effective acceleration due to increasing junction temperature of the laser) [14-22]. Equation (1) provides the acceleration of unreliability as a function of optical power, current and junction temperature, I is current, P is power, T_j is junction temperature, m is the acceleration parameter of optical power, n is the acceleration parameter of optical power, E_a is the activation energy and k_B is Boltzmann's constant.

$$\text{Acceleration Factor} \propto I^m P^n \exp\left(\frac{-E_a}{k_B \cdot T_j}\right) \quad (1)$$

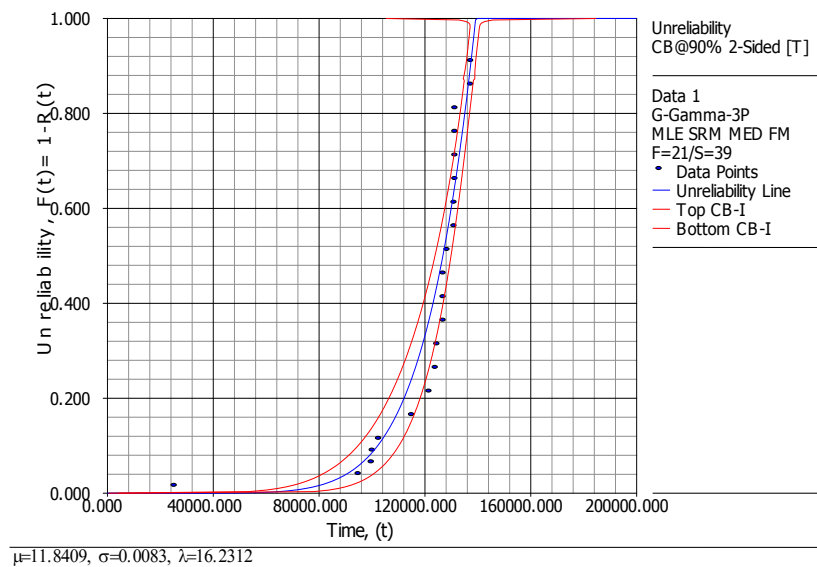
There has been very limited reports on the acceleration parameters from literature, especially for state-of-the-art devices near 80x nm wavelength [9-22]. In this paper, nominal parameters from literature, $m=2$ for current, $n=2$ for power, and $E_a=0.45\text{eV}$ for activation energy, were used. The calculated acceleration at 5 W 25 °C ($T_j \sim 64^\circ\text{C}$) is ~ 30 times comparing to 5W 25°C ($T_j \sim 38^\circ\text{C}$) operation. Using this acceleration, the equivalent time at 5W 25 °C ($T_j \sim 38^\circ\text{C}$) are plotted on the 2nd x axis for each group in Figure 5(a) and (b). As it is indicated, the 20 devices in Figure 5(a) have been life-tested well beyond 15 equivalent years at 5W 25 °C ($T_j \sim 38^\circ\text{C}$) operation.

Both random and wear-out failures with 95 μm stripes and 3.8mm cavities can be analyzed together in a mixed Weibull model and/or a Generalized Gamma model [23], and results are shown in Figure 6 with time converted to 5 W 25 °C ($T_j \sim 38^\circ\text{C}$) operation. The mixed Weibull distribution is a common model for analyzing the case of more than one failure mode, as each failure mode can be described with a distinct Weibull distribution. Generalized Gamma distribution is not very often used for life data analysis but it has the ability to mimic other distributions such as Weibull distribution. There are a total of 21 failures out of 60 devices on lifetests accumulate so far. Figure 6 has failures as individual dots and the center fitting curve representing 50% confidence, in (a) mixed Weibull distribution model (two subgroups) and (b) Generalized Gamma distribution model. Fitting with both models are pretty good. Two-sided 90% confidence bounds are also shown as two outlining curves around the center-fitting curve, in Generalized Gamma distribution model shown Figure 6(b). In the regime before wear-out onsite, the failure rate is low and time before 5% failure (B5) is calculated to

be > 9.7 years with 90% confidence, for 5W 25°C (Tj~38 °C) operation. The wear-out onset is also > 10 years of equivalent at 5 W 25 °C (Tj ~ 38 °C) operations.



(a)



(b)

Figure 6: Reliability analysis of lifetests on 95 μm stripes and 3.8 mm cavities, (a) Unreliability using mixed Weibull distribution model (two subgroups), (b) Unreliability with 90% confidence bounds using Generalized Gamma distribution model

A total of 61 devices with 200 μm stripes and 3.8 mm cavities have been tested under accelerated lifetest conditions. Samples of the accelerated lifetest data of HE devices with 200 μm stripes and 3.8 mm cavities are shown in Figure 7. In Figure 7(a), the 16 780nm devices have been running for about 3000 hours at 12 A and 50 °C heatsink temperature (Tj~67 °C), without showing wear-out behavior yet. There is also no sign of sudden failure or slow degradation. In Figure 7(b), the 13 808nm devices have been running passing 9000 hours at 14 A, and 50 °C heatsink temperature

($T_j \sim 71^\circ\text{C}$), with wear-out behavior at around 4000 hours. There is one single device sudden failure before wear-out. Using equation (1) and nominal parameters from literature, $m=2$ for current, $n=2$ for power, and $E_a=0.45\text{eV}$ for activation energy, the calculated acceleration at 12 A 50°C ($T_j \sim 67^\circ\text{C}$) and 14 A 50°C ($T_j \sim 71^\circ\text{C}$) is ~ 17 and ~ 38 separately, comparing to 8 W 25°C ($T_j \sim 44^\circ\text{C}$) operation. Using this acceleration, the equivalent time at 8W 25°C ($T_j \sim 44^\circ\text{C}$) are plotted on the 2nd x axis for each group in Figure 7 (a) and (b). As shown, the 13 devices in Figure 7(b) have been life-tested well beyond 40 equivalent years at 8 W 25°C ($T_j \sim 44^\circ\text{C}$) operations.

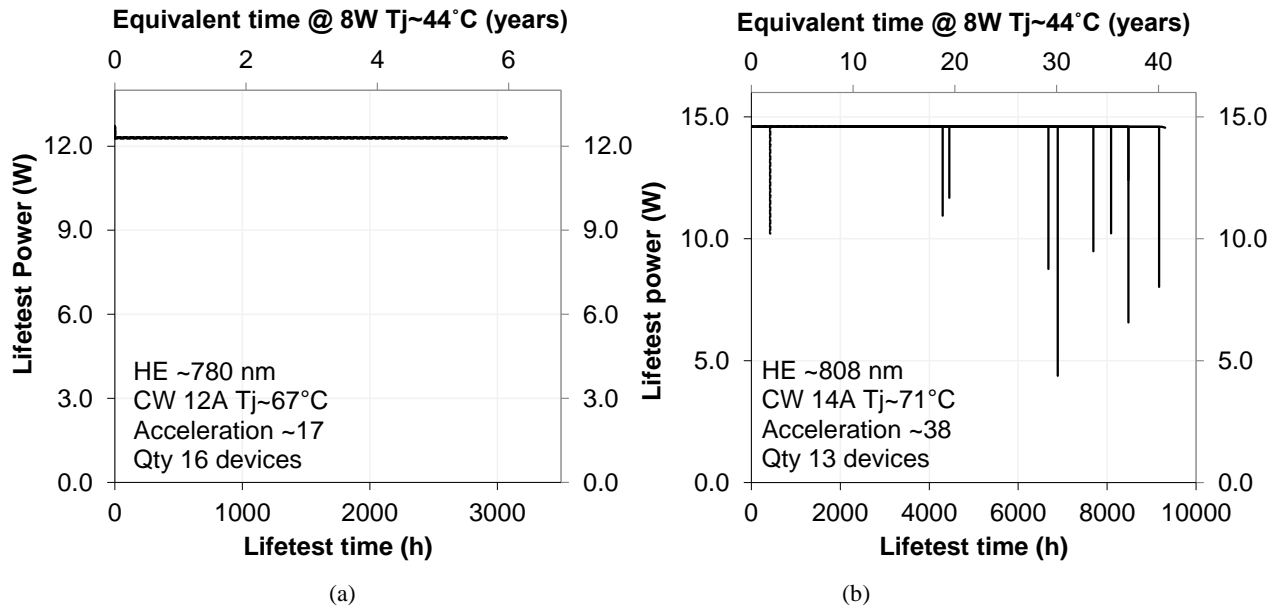
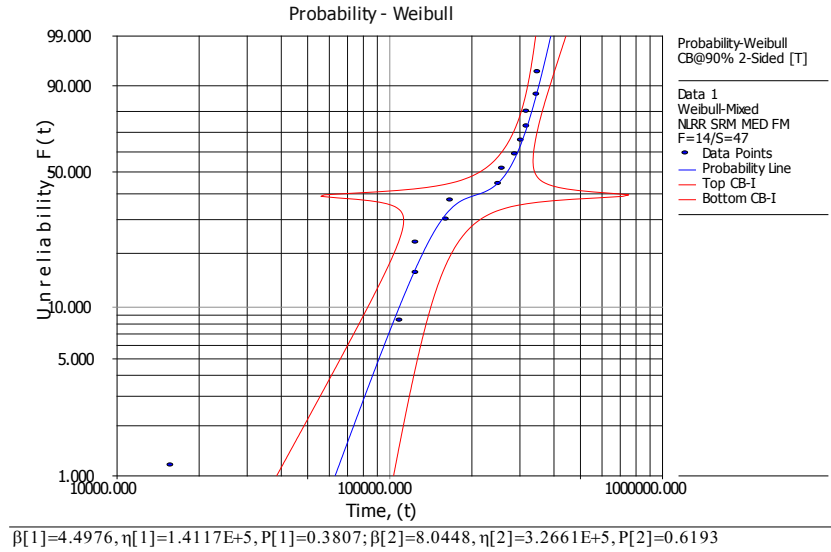
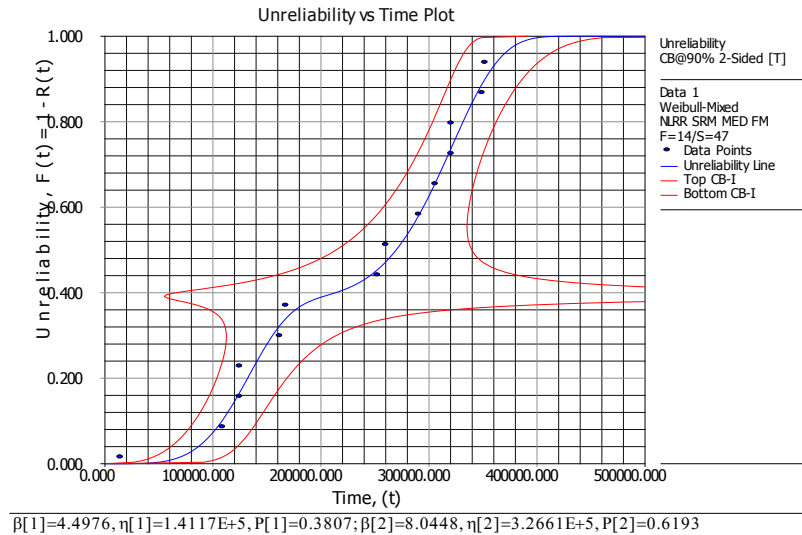


Figure 7: Accelerated lifetest on devices with $200\ \mu\text{m}$ stripes and $3.8\ \text{mm}$ cavities (a) 16 $780\ \text{nm}$ devices, at 12 A 50°C ($T_j \sim 67^\circ\text{C}$), with no failure and wear-out onset yet (b) 13 $808\ \text{nm}$ devices, at 14 A 50°C ($T_j \sim 71^\circ\text{C}$), tested to wear-out

The mixed Weibull model is used to analyze the distribution, and the results are shown in Figure 8, with time converted to 8 W 25°C ($T_j \sim 44^\circ\text{C}$) operation. There are a total of 14 failures out of 61 devices on lifetests collected so far. The best fitting is achieved with two subgroups, and two-sided 90% confidence bounds are also shown as two outlining curves around the center-50%-bound curve. The plots indicate more data at wear-out regime is needed to get better confidence on fitting in this regime, which could be a result of soft wear-out turn-on in Figure 7(b). In the regime before wear-out onsite, the failure rate is still low and time before 5% failure (B5) is calculated to be > 7.5 years with 90% confidence, for 8 W 25°C ($T_j \sim 44^\circ\text{C}$) operation. And the wear-out onset is also > 11 years of equivalent at 8 W 25°C ($T_j \sim 44^\circ\text{C}$) operations.



(a)



(b)

Figure 8: Reliability analysis of lifetest with mixed Weibull distribution model on 200 μm stripes and 3.8 mm cavities,,
(a) Probability with 90% confidence bounds, (b) Unreliability with 90% confidence bounds

Failure analysis was performed on all 35 failures identified so far. Two main failure modes: the COMD failure mode where failure originates from facet and bulk-defect initiated COD (BCOD) [12-13]. In the random failure regime, both BCOD (1 failure out of 121) and COMD (1 failure out of 121) have been observed. Failures after wear-out start are identified to be COMD only (33 failure out of 121). This is different than what we found on 9xx nm lasers, which do not show any COMD wear-out even with much higher power acceleration and much longer lifetest [15-16]. This also suggests that lasers with shorter wavelengths are likely more prone to COMD due to higher photon energy. Thus good facet passivation is essential for high reliability in 780-820 nm devices.

3. HIGH PERFORMANCE FIBER-COUPLED MODULES

High power reliable single emitter lasers are combined into nLight's compact, passively-cooled Pearl product architecture [24-28]. Each laser is individually collimated in the fast axis and slow axis and free-spaced coupled into a single fiber. Pearl modules are not subject to device cross heating and are thus able to operate at a very high power densities. The optics are designed to efficiently image the diode laser onto fiber, scale high power/ brightness and maintain high efficiency of the high power single emitter diode lasers. Besides the scaling of power and brightness in Pearl module, the reliability of the module is also further improved from the high reliable single emitter diode lasers by effective redundancy. Using P16 (16-emitter) module as an example, module failure is defined as the 4th sudden failure of laser happens inside the module (module power drops >20% of the initial power at a fixed current). Then the module reliability R_{module} can be described as a function of laser reliability R_{laser} as in binomial equation (2).

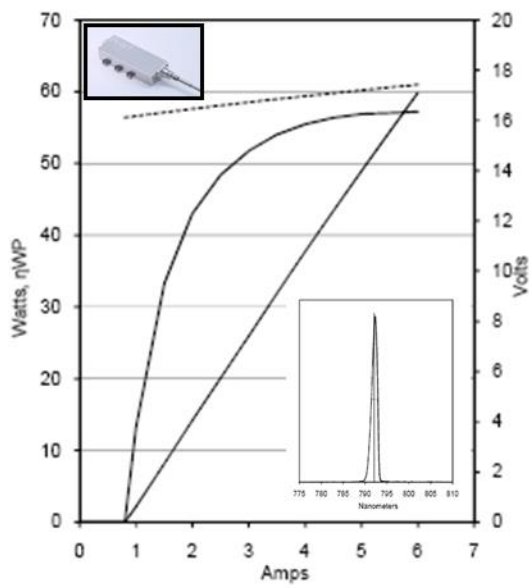
$$R_{\text{module}} = \sum_{i=0}^3 \frac{16!}{(16-i)!i!} \cdot R_{\text{laser}}^{16-i} \cdot (1 - R_{\text{laser}})^i \quad (2)$$

Laser FIT at 1000 means laser reliability is >98% by the end of 2 year uninterrupted operation. Using equation (2), module reliability can be calculated as 99.98% by the end of 2 year uninterrupted operation. This indicates that the reliability of modules based on reliable high power single emitter diode lasers is also greatly improved. So normally lasers can be operated with higher power/temperature in a Pearl product architecture with effective redundancy than in a single-emitter format, for the same reliability requirements. Table 1 listed module reliability for different modules with different redundancies, with the number of single emitter from 10 to 16, when chip reliability is ~98%.

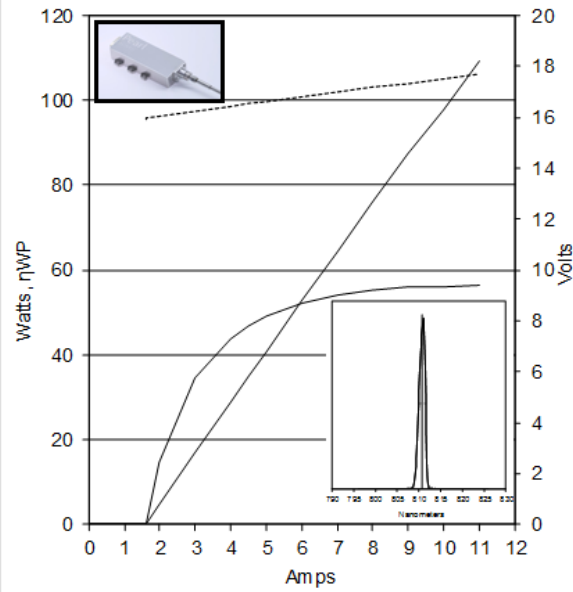
Pearl™ Reliability	1 redundancy	2 redundancy	3 redundancy
10 emitters	98.38%	99.91%	-
14 emitters	96.90%	99.75%	-
16 emitters	96.01%	99.63%	99.98%

Table 1: Module reliability for different modules with different redundancies, when chip reliability is ~98%.

Fiber-coupled pump Pearl modules from a 200 μm core fiber were developed with 10-emitter of 792 nm 95 μm diode lasers, with typical power and efficiency performance shown in Figure 1(a). When operated in CW mode at 30 $^{\circ}\text{C}$, these modules are capable of coupling over 50 W CW power into a 200 μm fiber with an NA of 0.18. Figure 9 (a) shows the LIV and spectrum characteristics of module performance, with threshold ~0.8 A and slope ~11.4 W/A. The peak efficiency is ~57% and efficiency at 50 W is around 56%. At 50 W 30 $^{\circ}\text{C}$, Full Width Half Maximum of the whole module is 1.5 nm, which is comparable to the single diode at the same working condition. Figure 9(b) shows the LIV and spectrum of module with 10-emitters of 810 nm 200 μm diode lasers, with a NA of 0.17 from a 400 μm core fiber. The module can be tested above 100W and power vs current is still very linear in this range. The threshold is ~1.6 A and slope ~11.8 W/A. The peak efficiency is ~57% and efficiency at 100 W is around 56%. At 70 W 25 $^{\circ}\text{C}$ CW operation, Full Width Half Maximum of the whole module spectrum is 1.7 nm, and Full Width 1/e² Maximum is ~2.6 nm.



(a)



(b)

Figure 9: LIV and spectrum from (a) 200 μm 0.18 NA 792 nm fiber-coupled module tested at 30 $^{\circ}\text{C}$, CW (b) 400 μm 0.17 NA 810 nm fiber-coupled module tested at 25 $^{\circ}\text{C}$, CW.

The key parameters are summarized in Table 2. The 10-emitter modules are rated 40 W with a 200 μm diameter core fiber (this architecture utilizes 95 μm stripe devices) and 70 W with a 400 μm diameter core fiber (this package utilizes the 200 μm stripe lasers). The modules are designed to operate at peak efficiency, which is $\sim 56\%$ regardless of configuration. This high efficiency is enabled by the excellent ($\sim 90\%$) overall optical-to-optical efficiency offered by the approach. A 16-emitter module utilizing 200 μm stripe devices and coupled to a 400 μm core fiber is rated to 120W.

Key Parameters	200 μm P10	400 μm P10	400 μm P16
Rated Power	40W	70W	120W
Peak efficiency	$\sim 56\%$	$\sim 56\%$	$\sim 56\%$
NA	< 0.22	< 0.22	< 0.22

Table 2: Module key parameters with HE single emitters

Figure 10 illustrates lifetesting results for four modules operating at 11 A, 36 $^{\circ}\text{C}$. Over 900 hours of failure-free operation has been recorded to date.

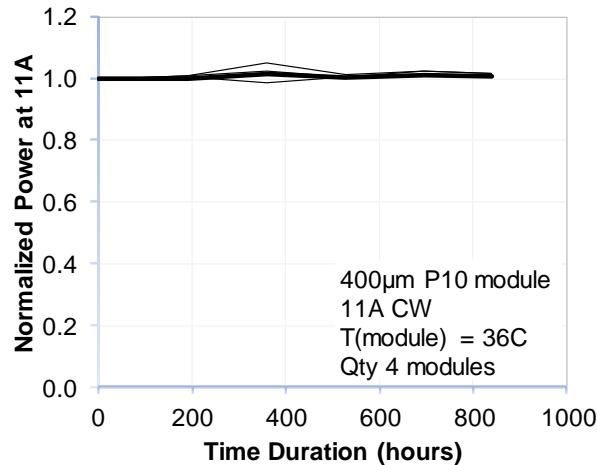


Figure 10: Accelerated lifetest for modules performed at 36 °C and 11 A driving current.

5. CONCLUSIONS

In summary, we present recent progress in the development of 95 µm and 200 µm stripe single emitter broad area diode lasers at 780-820 nm with high performance and high reliability. Initial performance and lifetest data support 95 µm stripe and 3.8mm cavity length single emitter broad area diode lasers at operation to 5 W. Similarly, 200 µm stripe and 3.8 mm cavity length single emitter broad area diode lasers can be rated to 8W reliable operation. These diode lasers have demonstrated higher efficiency (65%), higher brightness, narrow spectrum width, improved NF/FF control, than that of previous generation products. These advancements were enabled by application of design concepts originally developed for the 9xx nm wavelength band to the 780-820 nm wavelength range. Fiber-coupled modules based on arrays of these devices support >100W reliable operation, with a high 56% operating efficiency.

REFERENCES

- [1] Maik Frede, Ralf Knappe, and Dietmar Kracht, "250-W end-pumped Nd:YAG laser with direct pumping into the upper laser level," *Optics Letters*, 31, 3618(2006)
- [2] E. C. Sousa, I. M. Raniere, S. L. Baldochi, and N. U. Wetter, "Compact diode-side-pumped Nd:YLF laser with high beam quality, *AIP Conf. Proc.* 992, 426 (2008)
- [3] William F. Krupke, Raymond J. Beach, Vernon K. Kanz, Stephen A. Payne, and James T. Early, "New class of cw high-power diode-pumped alkali lasers (DPALs)," *Proc. SPIE* 5448, 7 (2004)
- [4] Adrian Carter, Bryce Samson, and Kanishka Tankala, "FIBER LASERS: Thulium-doped fiber forms kilowatt-class laser," *OptoIQ*, Apr 1(2009).
- [5] Peter F. Moulton, Glen A. Rines, Evgueni V. Slobodtchikov, Kevin F. Wall, Gavin Frith, Bryce Samson, and Adrian L. G. Carter "Tm-Doped Fiber Lasers: Fundamentals and Power Scaling," *IEEE J. Quantum Electron.* Vol. 15, No. 1, 85 (2009)
- [6] J. Wang, B. Smith, X. Xie, X. Wang and G. Burnham, "High-efficiency diode lasers at high output power", *Applied Physics Letters*, Vol. 74, No. 11, 1525 (1999)
- [7] P. Crump, W. Dong, M. Grimshaw, J. Wang, S. Peterson, D. Wise, M. DeFranza, S. Elim, S. Zang, M. Bougher, J. Peterson, S. Das, J. Bell, J. Farmer, M. DeVito, R. Martinsen, "100-W+ Diode Laser Bars Show >71% Power Conversion from 790-nm to 1000-nm and Have Clear Route to > 85%", *Proc. of SPIE* 6456, 645660M (2007)

- [8] A. Al-Muhanna, J. K. Wade, T. Earles, J. Lopez, and L. J. Mawst, "High-performance, reliable, 730-nm-emitting Al-free active region diode lasers," *Applied Physics Letters*, Vol. 73, No. 20, 2869 (1998).
- [9] M. Razeghi, H. J. Yi, J. E. Diaz, S. Kim, M. Erdtmann, "Temperature Insensitivity of the Al-free InGaAsP Lasers for $\lambda=808$ and 980 nm," *Proceedings of SPIE* 3001, 243 (1997).
- [10] K. Hausler, U. Zeimer, B. Sumpf, G. Erbert and G. Trinkle, "Degradation model analysis of laser diodes," *J. Mater Sci: Mater Electron* 19, 160 (2008)
- [11] V. Gapontsev, I. Berishev, V. Chuyanov, G. Ellis, I. Hernandez, A. Komissarov, N. Moshegov, O. Raisky, V. Rastokine, N. Strougov, P. Trubenko, L. Wright, and A. Ovtchinnikov, "8xx – 10xx nm Highly Efficient Single Emitter Pumps", *Proc. of SPIE* 6876, 68760I (2008)
- [12] V. Gapontsev, N. Moshegov, P. Trubenko, A. Komissarov, I. Berishev, O. Raisky, N. Strougov, V. Chuyanov, G. Kuang, O. Maksimov, and A. Ovtchinnikov* "High-brightness fiber coupled pumps", *Proc. of SPIE* 7198, 71980O (2009)
- [13] J. Wang, L. Bao, M. Devito, D. Xu, D. Wise, M. Grimshaw, W. Dong, S. Zhang, C. Bai, P. Leisher, D. Li, H. Zhou, S. Patterson, R. Martinsen and J. Haden, "Reliability and Performance of 808nm Single Emitter Multi-Mode Laser Diodes," *Proc. of SPIE* 7583, 758305 (2010).
- [14] Ling Bao, Jun Wang, Mark Devito, Dapeng Xu, Mike Grimshaw, Weimin Dong, Xingguo Guan, Hua Huang, Paul Leisher, Shiguo Zhang, Damian Wise, Rob Martinsen, and Jim Haden, "Performance and Reliability of High Power 7xx nm Laser Diodes," *Proc. of SPIE* 7953, (2011).
- [15] L. Bao, J. Wang, M. DeVito, D. Xu, D. Wise, P. Leisher, M. Grimshaw, W. Dong, S. Zhang, K. Price, D. Li, C. Bai, S. Patterson, R. Martinsen, "Reliability of High Performance 9xx-nm Single Emitter Diode Lasers," *Proceedings of SPIE* 7583, 758302 (2010).
- [16] Ling Bao, Paul Leisher, Jun Wang, Mark Devito, Dapeng Xu, Mike Grimshaw, Weimin Dong, Hua Huang, Shiguo Zhang, Damian Wise, Rob Martinsen, and Jim Haden "High Reliability and High Performance of 9xx-nm Single Emitter Laser Diodes," *Proceedings of SPIE* 7918, 7918-05 (2011).
- [17] V. Rossin, E. Zucker, M. Peters, M. Everett and B. Acklin, "High-Power High-Efficiency 910-980nm Broad Area Laser Diodes," *Proc. of SPIE* 5336, 5336-27 (2004).
- [18] Z. Yao, E. Zucker, K. Uppal, D. Coblentz, P. Liang, K. Peters, and R. Craig, "High power and high reliability InGaAs broad area lasers emitting between 910 and 980 nm," *Lasers and Electro-Optics Society 2000 Annual Meeting. LEOS 2000. 13th Annual Meeting. IEEE*, vol. 2, 510 (2000).
- [19] T. Strite, "High Reliability Diode Pump Lasers," *IEEE SCV LEOS Chapter Meeting*, <http://www.jdsu.com/products/optical-communications/technology-presentations.html> (2007).
- [20] Y. Zou, E. Zucker, K. Uppal, D. Coblentz, P. Liang, M. Peters and R. Craig, "Reliability and Performance of InGaAs Broad Area Lasers Emitting Between 910 – 980 nm," *Proc. SPIE* 4285, 159 (2001)
- [21] M. Kanskar, M. Nesnidal, S. Meassick, A. Goulakov, E. Stiers, Z. Dai, T. Earles, D. Forbes, D. Hansen, P. Corbett, L. Zhang, T. Goodbough, L. LeClair, N. Holehouse, D. Botez and L.J. Mawst, "Performance and Reliability of ARROW Single Mode & 100 μ m Laser Diode and the Use of NAM in Al-free Lasers," *Proc. of SPIE* 4995, 196 (2003).
- [22] J. Van de Castele, M. Bettiati, F. Laruelle, V. Cargemel, P. Pagnod-Rossiaux, P. Garabedian, L. Raymond, D. Laffitte, S. Fromy, D. Chambonnet and J. P. Hirtz, "High reliability level on single-mode 980 nm-1060 nm diode lasers for telecommunication and industrial applications", *Proc. of SPIE* 6876, 68760P (2008)
- [23] ReliaSoft ALTA, <http://www.reliasoft.com/alta/index.htm>.
- [24] D. Schulte, Y. Yan, R. J. Martinsen, A. L. Hodges, S. R. Karlsen, "Modular diode laser assembly," US Patents 7420996, 7436868, and 7443895.
- [25] S. R. Karlsen, R. K. Price; M. Reynolds, A. Brown, R. Mehl, S. Pattern, R. J. Martinsen, "100-W, 105- μ m, 0.15NA Fiber Coupled Laser Diode Module," *Proc. of SPIE* 7198, 71980T(2009).

- [26] S. Patterson, "Advances in High Power, High Efficiency, High Brightness Fiber Coupled Diode Lasers from 635-nm to 1900-nm and Beyond," 20th Annual Solid State and Diode Laser Technology Review, (2007).
- [27] K. Price, S. Patterson, S. Karlsen, A. Brown, R. Mehl, R. Martinsen, K. Kennedy, D. Schutle, and J. Bell, "Progress in Fiber-Coupled, High-Brightness, High-Power Diode Laser Pump Sources," SSDLTR (2008)
- [28] K. Price, S. Karlsen, P. Leisher, R. Martinsen, "High Brightness Fiber Coupled Pump Laser Development," Proc. of SPIE 7583, 758308 (2010).